Relativistic NN scattering calculations with Δ degrees of freedom

E. E. van Faassen
Institute for Theoretical Physics, University of Utrecht, 3508 TA Utrecht, The Netherlands

J. A. Tjon*
Physics Department, University of Maryland, College Park, Maryland 20742
(Received 26 March 1984)

The Bethe-Salpeter equation for NN-NΔ scattering is extended to include ΔΔ states also. With the exception of $^1S_0$, the effects are small for $T=1$ because of dominance by NΔ isobaric states. For $T=0$ the influence is accordingly larger. Also a quasipotential approximation to the Bethe-Salpeter equation is considered. Substantial differences are found. In particular, the quasipotential results are considerably more sensitive to the coupling parameters of the transition interaction. As a result a better fit to existing experimental phase shift parameters is obtained with the Bethe-Salpeter equation.

I. INTRODUCTION

Recent years have witnessed great efforts to extend conventional NN scattering theories to include extra degrees of freedom.[1–3] Interest has centered around the pion and its production mechanism via Δ isobar doorway states. Effects from coupling to these inelastic channels are obviously required for a reliable description of the intermediate energy region up to 1 GeV. Investigation of these states is closely connected to the controversy over the existence of possible dibaryon resonances.[4] The latter were proposed after NN scattering polarization experiments revealed rich energy and spin dependence at intermediate energies.[5] Since then, however, it has been shown that a conventional mechanism like coupling to NNπ (Refs. 6–10) or isobar channels[11–15] could account for these structures as well.

Previous work (Refs. 16 and 17, hereafter referred to as I) showed that a reasonable description of NN scattering in the isospin 1 channel for laboratory energies up to 1 GeV can be given with a Bethe-Salpeter equation (BSE) by including Δ degrees of freedom. One of the main motivations for using the coupled channel ladder BSE as the dynamical equation lies in the possibility of modifying the relativistic propagators to also include the contributions from NNπ inelastic channels. As a result such a model can account in an appropriate way for the pion production processes.

In this paper we study two separate problems: First, we extend the existing NN↔NΔ model to include ΔΔ channels. This allows consideration of isospin zero channels also. The additional algebra and details of its numerical solution are presented in Sec. II.

Second, we repeat these calculations in a quasipotential approximation. This allows a better comparison with several three-body models which have been presented so far. The nature of this approximation and its numerical implementation are described in Sec. III. Section IV gives the results from both methods. A BSE variant taking into account the composite nature of the Δ is presented in Sec. V.

Some concluding remarks are made in Sec. VI, followed by two appendices giving details about the partial wave reduction and some comments on the Δ-propagator used.

II. INCLUSION OF THE ΔΔ CHANNELS

Since the Δ isobar carries isospin $\frac{3}{2}$, it can be excited from the nucleon by isovector mesons only, the two candidates being the pseudoscalar pion and vector rho meson. Comparing NΔ and ΔΔ thresholds of 640 and 1400 MeV we expect ΔΔ states to be of minor importance for isospin 1 channels. For isospin 0 they may be an important source of inelasticity, however, due to the absence of NΔ states. As before, ΔΔ vertices were disregarded in view of the uncertainties about their form.

The resulting BSE is represented diagrammatically in Fig. 1. In accordance with the notation of I we use a subscript $i=1$, 2, and 3 to label NN, NΔ, and ΔΔ states, respectively. Going through the partial wave reduction and Wick rotation we arrive at a BSE almost identical to Eq. (17) of I:

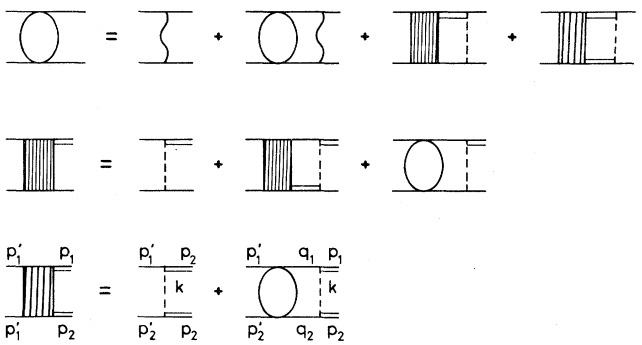

FIG. 1. Diagrammatic representation of the Bethe-Salpeter equation for coupled channel NN + NΔ + ΔΔ scattering. The dashed line indicates π+ρ exchange, the wiggly line stands for combined π, η, ϵ, δ, ρ, and ω exchange.

$$\tilde{\Phi}_1(ip_0pJL'S')={}_i\langle ip_0pJL'S' \mid \tilde{V} \mid 0\hat{p}JLS\rangle_1$$
$$+\frac{1}{2\pi^2}\sum_{j=1}^{3}\sum_{\tilde{L}\tilde{S}}\int_{-\infty}^{-\infty}dq_0\int_0^{\infty}dq\,{}_i\langle ip_0pJL'S' \mid \tilde{V} \mid iq_0qJ\tilde{L}\tilde{S}\rangle_j D_j(iq_0q)\tilde{\Phi}_j(iq_0qJ\tilde{L}\tilde{S})$$
$$+\frac{1}{\pi}\sum_{\tilde{L}\tilde{S}}\int_0^{\hat{p}}dq[{}_i\langle ip_0pJL'S' \mid \tilde{V} \mid -\alpha(q)qJ\tilde{L}\tilde{S}\rangle_1+{}_1\langle ip_0pJL'S' \mid \tilde{V} \mid [\alpha(q)qJ\tilde{L}\tilde{S}\rangle_1]R_1(q)\tilde{\Phi}_1[\alpha(q)qJ\tilde{L}\tilde{S}]$$
$$+\frac{1}{\pi}\sum_{\tilde{L}\tilde{S}}\int_0^{\hat{p}}dq\,{}_i\langle ip_0pJL'S' \mid \tilde{V} \mid \alpha(q)qJ\tilde{L}\tilde{S}\rangle_2 R_2(q)\tilde{\Phi}_2[\alpha(q)qJ\tilde{L}\tilde{S}]\,. \tag{1}$$

Here $\alpha(q)\equiv E-E_q+i\eta$ is the nucleon number two pole position. The only difference is in the double integral, where the sum over the virtual states now runs to three to include $\Delta\Delta$ states also. The single integral is due to the Wick rotation which picks up contributions from the propagator poles in the first and third quadrants of the q_0 plane. As before we restrict our attention to laboratory energies below 1 GeV up to which energies the Δ poles remain in the second and fourth quadrants. Consequently, there is no contribution from $\Delta\Delta$ states to the single integral.

The integral equation (1) is supplemented by an auxiliary equation for $\tilde{\Phi}_j[\alpha(p),p,JLS]$ with $j=1$ or 2. This equation has the same form as Eq. (1) with the argument ip_0 replaced by $\alpha(p)$.

In I the $N\Delta\pi$ and $N\Delta\rho$ interaction Lagrangians were given and the resulting $N\Delta$ transition amplitudes V_{12}, V_{21}, and V_{22} derived. We again choose the center of mass (c.m.) kinematics to be (see Fig. 1)

$$q_1=(E+q_0,\vec{q}),\quad p_1=(E+p_0,\vec{p}),\quad p_1'=(E+p_0',\vec{p}\,'),$$
$$q_2=(E-q_0,-\vec{q}),\quad p_2=(E-p_0,-\vec{p}), \tag{2}$$
$$p_2'=(E-p_0',-\vec{p}\,'),\quad k=p_1-q_1,\quad E^2=\frac{s}{4}\,.$$

Adopting the helicity formalism of Jacob and Wick[18] we introduce $U(V)$ and $\Delta(D)$ as the nucleon or delta spinors of particle number one (two). Explicit expressions for these helicity states have been given in Appendix A of I. Omitting the isospin factors, the $NN\leftrightarrow\Delta\Delta$ transition amplitudes are

(A) Pion exchange:

$$V_{13}=\frac{-f_{\pi\Delta}^2}{4\pi m_\pi^2}k_\mu\bar{\Delta}^\mu(\vec{p}_1)U(\vec{q}_1)k_\nu\bar{D}^\nu(\vec{p}_2)V(\vec{q}_2)\frac{1}{k^2-m_\pi^2}\,, \tag{3}$$

$$V_{31}=\frac{-f_{\pi\Delta}^2}{4\pi m_\pi^2}\bar{U}(\vec{p}_1)\Delta^\mu(\vec{q}_1)k_\mu\bar{V}(\vec{p}_2)D^\nu(\vec{q}_2)k_\nu\frac{1}{k^2-m_\pi^2}\,. \tag{4}$$

(B) Rho exchange:

$$V_{13}=\frac{f_{\rho\Delta}^2}{4\pi m_\rho^2}\frac{1}{k^2-m_\rho^2}\bar{\Delta}^\nu(\vec{p}_1)\gamma^\mu\gamma^5U(\vec{q}_1)\bar{D}^\rho(\vec{p}_2)\gamma^\sigma\gamma^5V(\vec{q}_2)$$
$$\times(k_\nu k_\sigma g_{\mu\rho}+k_\rho k_\mu g_{\nu\sigma}-k_\mu k_\sigma g_{\nu\rho}-k_\nu k_\rho g_{\mu\sigma})\,, \tag{5}$$

$$V_{31}=\frac{f_{\rho\Delta}^2}{4\pi m_\rho^2}\frac{1}{k^2-m_\rho^2}\bar{U}(\vec{p}_1)\gamma^5\gamma^\mu\Delta^\nu(\vec{q}_1)\bar{V}(\vec{p}_2)\gamma^5\gamma^\sigma D^\rho(\vec{q}_2)$$
$$\times(k_\nu k_\sigma g_{\mu\rho}+k_\rho k_\mu g_{\nu\sigma}-k_\mu k_\sigma g_{\nu\rho}-k_\nu k_\rho g_{\mu\sigma})\,. \tag{6}$$

Each transition amplitude carries an additional isospin factor of $-\sqrt{2}$ for $T=0$, $\sqrt{10/9}$ for $T=1$, and 0 for $T>1$ ($\Delta\Delta$ states with isospin $T=2,3$ are obviously inaccessible for NN scattering).

As in the previous work the singular behavior of the amplitudes is regularized by form factors F. These consist of two separate factors, one from each vertex:

$$F=F_1F_2\,, \tag{7}$$

$$F_1=\begin{cases}\left[\dfrac{\Lambda_{N\Delta}^2}{\Lambda_{N\Delta}^2-k^2}\right]^2 & \text{for N}\Delta\text{ vertices}\\[2ex] \dfrac{\Lambda_N^2}{\Lambda_N^2-k^2} & \text{for NN vertices}\end{cases}\,. \tag{8}$$

This entails a stronger regularization of the $NN\leftrightarrow N\Delta$ interaction than in I, where a monopole form factor was employed. The reason for not using monopole form factors is that the high momentum components of the $NN\leftrightarrow\Delta\Delta$ interaction lead to abnormally strong effects.

The definitions for obtaining the partial wave amplitudes from the spinor amplitudes Eqs. (3)—(6) are given in I [Eqs. (31) and (32)]. The procedure involves angular integration over rotation matrices for higher helicity values than the earlier $N\Delta$ case. The reduction of these new rotation matrices into a sum of Legendre polynomials is given in Appendix A.

The analytical expressions for the integrated spinor amplitudes were computed with the SCHOONSCHIP program for algebraic manipulation.[19]

The resulting expressions were verified to satisfy time reversal invariance

$${}_i\langle p_0pJL'S' \mid V \mid q_0qJLS\rangle_j={}_j\langle q_0qJLS \mid V \mid p_0pJL'S'\rangle_i \tag{9}$$

and to comply with the bounds on the partial wave transition amplitudes near threshold (i.e., either for q or $p\to 0$)

$${}_i\langle p_0pJL'S' \mid V \mid q_0qJLS\rangle_j=\mathcal{O}\left[p^{L'+2}q^{L+2}\right]\,. \tag{10}$$

Under the particle exchange operator P_{12} the $\Delta\Delta$ states transform just like NN states (the following relation does

not hold for NΔ states):

$$P_{12}|p_0pJLS\rangle_i=(-)^{L+S+T}|-p_0pJLS\rangle_i \quad i=1 \text{ or } 3 \quad (11)$$

where T is the total isospin. Just as in the NN case, the ΔΔ states with odd parity in the relative energy variable are neglected, the motivation being that they vanish in the nonrelativistic limit. For the NN problem this approximation has been shown to be reliable[20] in the elastic region. From Eq. (11) it is seen that the surviving states have odd values for $L+S+T$. For these channels particle exchange symmetry is satisfied automatically.

Furthermore, the NΔ-interaction Lagrangians have been chosen invariant under space reflection. The physical states (i.e., those surviving in the nonrelativistic limit) therefore separate into two classes of definite signature $(-)^I$, the NN and ΔΔ states moreover having odd $L+S+T$. For a given total angular momentum these two classes are given in Tables I and II. From these we see that we are left with at least five [parity group $(-)^J$, isospin 0], and at most twelve channels [parity group $(-)^{J+1}$, isospin 1]. For lower angular momenta several NΔ or ΔΔ states obviously cannot be realized, however.

For the ΔΔ propagator in Eq. (1) we used the analog of the positive energy propagators defined in I:

$$D_3^{-1}(q_0q)=[E+q_0-\hat{E}_3(q)+i\eta][E-q_0-\hat{E}_3(q)+i\eta] . \quad (12)$$

Here $\hat{E}_3(q)$ is the (complex) Δ energy in ΔΔ channels. This form is not obvious in view of the relativistic Δ propagator normally used. The approximations leading to Eq. (12) are studied in Appendix B for a very crude model of the NΔ box diagram. As before, pion production is simulated by giving the Δ mass a negative imaginary part Γ_3 (the subscript indicating that it is being used in the ΔΔ propagator):

$$\hat{E}_3(q)=(\mu_\Delta^2+q^2)^{1/2} ,$$
$$\mu_\Delta=m_0-\frac{i}{2}\Gamma_3(q) , \quad (13)$$

TABLE I. Quantum numbers for spatial parity $(-)^J$ (S,L,T)=(spin, orbital angular momentum, isospin).

		S	L	T Even J	T Odd J
1	NN	0	J	1	0
2	NN	1	J	0	1
3	NΔ	1	J	1	
4	NΔ	2	$J-2$	1	
5	NΔ	2	J	1	
6	NΔ	2	$J+2$	1	
7	ΔΔ	0	J	1	0
8	ΔΔ	1	J	0	1
9	ΔΔ	2	$J-2$	1	0
10	ΔΔ	2	J	1	0
11	ΔΔ	2	$J+2$	1	0
12	ΔΔ	3	$J-2$	0	1
13	ΔΔ	3	J	0	1
14	ΔΔ	3	$J+2$	0	1

TABLE II. Quantum numbers for spatial parity $(-)^{J+1}$.

		S	L	T Even J	T Odd J
1	NN	1	$J-1$	1	0
2	NN	1	$J+1$	1	0
3	NΔ	1	$J-1$	1	
4	NΔ	1	$J+1$	1	
5	NΔ	2	$J-1$	1	
6	NΔ	2	$J+1$	1	
7	ΔΔ	1	$J-1$	1	0
8	ΔΔ	1	$J+1$	1	0
9	ΔΔ	2	$J-1$	0	1
10	ΔΔ	2	$J+1$	0	1
11	ΔΔ	3	$J-3$	1	0
12	ΔΔ	3	$J-1$	1	0
13	ΔΔ	3	$J+1$	1	0
14	ΔΔ	3	$J+3$	1	0

with $m_0=1236$ MeV. For NΔ intermediate states with width Γ_2 was made a function of the maximum invariant energy $S_{\pi N}^{1/2}$ available in the presence of the spectator nucleon

$$S_{\pi N}=(\sqrt{s}-m)^2 \text{ for NΔ channels} , \quad (14)$$

where m is the nucleon mass. This prescription ensures that the Δ width Γ_2 in NΔ channels vanishes below pion production threshold at 287 MeV. For ΔΔ intermediate states, however, the spectator particle by itself is a πN system, yielding a different value of $S_{\pi N}$

$$S_{\pi N}=(\sqrt{s}-m-m_\pi)^2 \text{ for ΔΔ channels} . \quad (15)$$

Equation (15) leads to a threshold for Γ_3 which coincides with the physical NNππ threshold at 595 MeV. The values of Γ_2 and Γ_3 as functions of the laboratory energy are plotted in Fig. 2. Further remarks on the choice of Eq. (15) will be made in Sec. IV.

The integral equation (1) together with its auxiliary equation is solved in the same way as in I by iteration and

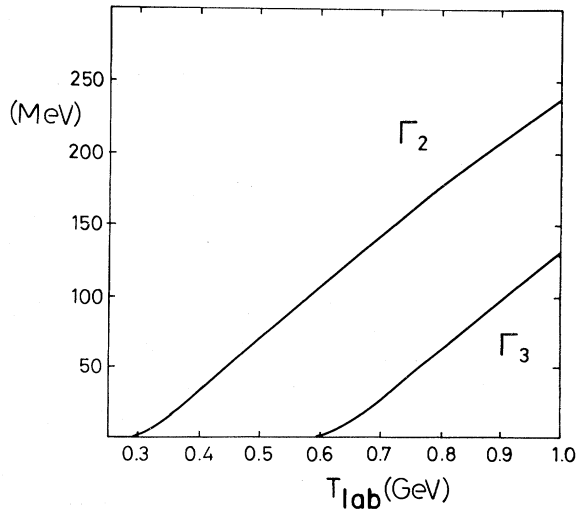

FIG. 2. Effective Δ width in NΔ channels (Γ_2) and ΔΔ channels (Γ_3) as function of laboratory energy.

construction of a Padé approximant to the Born series. In the numerical implementation the nucleon pole singularities were coped with by a subtraction in the NN channels. The single integral was done by Gaussian mesh points on the integral $[0,\hat{p}]$. As noted in I, the driving force in this integral can become complex for energies above pion production threshold. The ensuing integral over the imaginary interval was done with the same number of Gaussian mesh points. It was found that its points provided very good accuracy for the single integral (accuracy of box diagram better than 0.5%).

The double integral was done exactly as in Ref. 21, except that eight points were used in the q_0 integration (against twelve in Ref. 21). Trying various meshes for $^1D_2$ (which has a strong coupling to a singlet NΔ state) we found changes of about 1% in the box integral and considered this accuracy sufficient.

III. THE QUASIPOTENTIAL APPROXIMATION

In order to allow a comparison between our relativistic BSE results and those from a nonrelativistic potential model, it is natural to take a quasipotential model into consideration. Considering the pure NN case first, there is a well-known ambiguity in the reduction of the four-dimensional BSE to a relativistic three-dimensional scattering equation. Two classes are favored in the literature, both involving a delta-function prescription for the troublesome relative energy variable in the loop integral. The Gross-type model[22] comprises the positive energy pole contribution from the two particle propagator, thereby omitting contributions to the q_0 integration from the negative energy pole, the meson poles of the driving force, and possible cuts in the T matrix itself.

The Gross two particle propagator therefore is proportional to $\delta(q_0-E+E_2)$, where $E_2=(m_2^2+q^2)^{1/2}$ is the energy of particle number two with three momentum $\vec{q}$. The Blankenbecler-Sugar–type[23] two particle propagator is proportional to

$$\delta[q_0-(E_1-E_2)/2]$$

which reduces to $\delta(q_0)$ for the equal mass case. Other approximations like Thompson[24] or Kadychevsky[25] differ in the proportionality factor, but the δ function basically belongs to one of these two possibilities. For our coupled channel approach the use of these δ functions in the various channels leads to complex transition potentials,[26] however. Physically this reflects the possibility of the decay process $\Delta\rightarrow N+\pi$ for some values of incoming and outgoing momenta. The potentials being independent of the total c.m. energy $2E$, we would end up with unitarity violation below the first pion production threshold. To be more explicit we observe that with the Gross prescription the NN↔NN and NN↔NΔ potentials are both real as desired: For NN as well as NΔ states the second particle is a nucleon and the on shell condition for the pion

$$(E_p-E_q)^2-(\vec{p}-\vec{q}\,)^2-m_\pi^2=0 \tag{16}$$

can obviously not be satisfied.

Difficulties are caused by ΔΔ states, where the second particle now is a heavier Δ and the potential becomes complex. For a Blankenbecler-Sugar approach the same reasoning shows that the NN↔NΔ potential would become complex. A way out of this problem is to make the static approximation in all channels.[27–29] This yields real potentials.

Just as in the BSE case, pion production then will be taken into account by using a complex Δ mass in the Δ propagator. Explicitly, the two particle propagators $S_i(q_0q)$ are approximated as

$$S_i(q_0q)=D_i(q_0,q)\sum_{\sigma_1}u\bar{u}\sum_{\sigma_2}v\bar{v} \tag{17}$$

$$\rightarrow 2\pi i Q_i(q)\delta(q_0)\sum_{\sigma_1}u\bar{u}\sum_{\sigma_2}v\bar{v}\,. \tag{18}$$

Here u and v are the particle number 1 and 2 spinors, respectively. They can be N or Δ spinors depending on the channel index i. The quasipotential propagators Q_i are defined as

$$\begin{aligned} Q_1^{-1}(q)&=2(E_q-E)\,,\\ Q_2^{-1}(q)&=E_q+\hat{E}_2(q)-2E\,,\\ Q_3^{-1}(q)&=2[\hat{E}_3(q)-E]\,. \end{aligned} \tag{19}$$

As before, the complex delta mass depends on the channel involved since different Δ widths Γ_2 and Γ_3 are used in NΔ and ΔΔ channels, respectively (cf. Sec. II). The quasipotential analog of the BSE then becomes

$$\tilde{\Phi}_i(p,JL'S')={}_i\langle 0pJL'S'\mid\tilde{V}\mid 0\hat{p}JLS\rangle_1+\frac{1}{\pi}\sum_{j=1}^{3}\int_0^\infty dq\,{}_i\langle 0pJL'S'\mid\tilde{V}\mid 0qJ\tilde{L}\,\tilde{S}\rangle_j Q_j(q)\tilde{\Phi}_j(qJ\tilde{L}S)\,. \tag{20}$$

In this equation the driving force $\tilde{V}$ is identical to that used in Eq. (1) with relative energy variables set to zero. Equations (19) show that the NN propagator $Q_1(q)$ develops a pole at $q=\hat{p}$, where $E=(m^2+\hat{p}^2)^{1/2}$. Therefore a subtraction is required in the intermediate NN channels. The two other propagators do not develop poles near the line of integration due to the Δ mass becoming complex, thus obviating the need for a subtraction in these channels. Equation (20) is solved by the same method as the full BSE: Padé approximants are constructed for the Born series of the integral equation. The integration interval was divided into three parts: The first two were $[0,\hat{p}]$ and $[\hat{p},2\hat{p}]$ containing n_1 Gaussian mesh points each. The remaining half-line $q>2\hat{p}$ was mapped on the interval $[0,1]$ by defining

$$q(x)=2\hat{p}-2\log x,\quad \text{for } x\in[0,1] \tag{21}$$

where n_2 Gaussian x points were chosen on the unit interval. It was found that numerical stability was obtained with $n_1=4$, $n_2=8$.

IV. RESULTS

All BSE results were obtained with the same parameter set, which is given in Table III. Before turning to $\Delta\Delta$ states we briefly discuss the effect of the stronger regularization for the NN↔NΔ amplitudes. In comparison with previous calculations the largest changes occurred not surprisingly in channels with the highest sensitivity for the NΔ cutoff mass $\Lambda_{N\Delta}$: The phase shift of $^1D_2$ was lowered towards experimental results (this particular channel couples to an S-wave NΔ channel). Similarly $^3P_2$ is reduced about 4 deg over the whole energy range 200—1000 MeV. The change in the remaining isospin 1 channels is negligible. With regard to inelasticities the prominent cutoff dependent humps for $^3P_0$ and $^3P_1$ have vanished. Understandably the dependence on $\Lambda_{N\Delta}$ is reduced strongly. For reference, results from the old cutoff procedure have been included in Fig. 3 only when justified by a significant change. The parametrization used is that of Arndt and VerWest,[30] and has been given in Eqs. (45) and (46) of I.

Figures 3 and 4 show the effects of $\Delta\Delta$ states. Prominent changes occur for $^1S_0$, where a strong coupling from the S wave $\Delta\Delta$ channel was expected. The weak coupling to the D-wave NΔ channel introduced only a small inelasticity. Therefore the effect of the Γ_3 threshold at 595 MeV is very large. A choice different from Eq. (5) results in a steep rise in inelasticity from the new threshold. This explains the absence of a notable inelasticity from $^1S_0$ in the results of Ref. 9. In this model the spectator system is considered a bare Δ instead of a π-N system as we did.

The corresponding threshold for pion production from $\Delta\Delta$ states is located at $T_{\rm lab}\sim 970$ MeV, just bordering the energy region considered. This ambiguity in the prescription for Γ_3 clearly points out the need for a pion production mechanism which is more systematic than our parametrization with an energy-dependent width.

In this context it is necessary to make some comments on the sensitivity of the inelasticity on the value of Γ_2. As mentioned in I different parametrizations of Γ_2 did not produce appreciably different results. It turns out, in fact, that, once Γ_2 is larger than about 60 MeV, there is only a very modest influence on either phase shift or inelasticity. This can be seen from Table IV which shows results of a NN + NΔ channel calculation in the quasipotential approximation (cf. Sec. III). Only isospin 1 channels were considered. With the existing programs it is not possible to determine the value of Γ_2 at which the inelasticity begins to decrease ($\lim\Gamma_2\to 0$ brings the pole in the NΔ propagator near the line of integration, making an additional subtraction necessary). Similar conclusions hold for the BSE also, although we restricted calculations to a few cases in view of the required computing time: At 800 MeV laboratory energy the standard value of Γ_2 is about 176 MeV. Reduction to 60 MeV resulted in modest changes comparable to those in Table IV. Stability of the BSE integration at $\Gamma_2=60$ MeV was verified for the NN + NΔ box diagram.

This rapid saturation of inelasticity explains why $\Delta\Delta$ channels fail to increase the NΔ-induced inelasticities for isospin 1 channels, with exception of $^1S_0$. Apart from this channel, $^3P_2$ is the only other $T=1$ channel where additional attraction from the (closed) $\Delta\Delta$ channels manifests itself. The shift is about 4 deg towards experimental data, and (accidentally) compensates the fact that we used a stronger cutoff on the NN↔NΔ amplitudes than in previous work.

For isospin zero the situation is different due to the absence of NΔ channels with their associated inelasticity. Greatest attraction is seen to occur in the strongly interacting S wave. The absence of sizable effects from $^3D_2$ is remarkable in view of its coupling to an S wave $\Delta\Delta$ channel. Comparing with phase shifts from the nonrelativistic calculations of Holinde and Machleidt[31] below pion threshold, we find good agreement for isospin 1 channels. Differences occur for $T=0$ states. For $^3S_1$ their prediction of 22 deg additional attraction is twice the amount we find. This is surprising in view of their using a smaller cutoff mass at 1200 MeV. In contrast to this our additional attraction in $^1P_1$ is about twice the Holinde-Machleidt result. Moreover, keeping only NN intermediate states we already find too much attraction as compared to experimental data. It indicates that the NN↔NN part of the interaction in the $^1P_1$ state is not described well. This particular channel is strongly dependent on virtually every parameter in our model. We therefore expect that more refined calculations will lead to a better agreement.

Figures 4 and 5 show analogous results for the quasipotential model of Eq. (20). The parameters of the BSE lead to unstable Padé series and have to be modified. First, the cutoff masses have to be reduced to $\Lambda^2_{NN}=1.5$, $\Lambda^2_{N\Delta}=1.3$. Reference 20 was used as a guide for the choice of the coupling constants, which have been listed in Table III also. The requirement of reducing the cutoff masses is symptomatic for the greater sensitivity of the QP model on various parameters. The ρNΔ coupling constant, for instance, has to be taken 1.0, in sharp contrast to the values of 8.0 used in BSE and 10.33 expected from quark model considerations. if we had used 8.0 instead, the pseudoresonance structures in $^1D_2$ and $^3F_3$ would have been suppressed considerably. Furthermore, $^3P_2$ would have become much too attractive. The wish to retain resonancelike structures motivated us to resort to a weak

TABLE III. Coupling constants used in the Bethe-Salpeter and quasipotential equations. The cutoff masses are expressed in nucleon masses.

	$\frac{g_\pi^2}{4\pi}$	$\frac{g_\delta^2}{4\pi}$	$\frac{g_\eta^2}{4\pi}$	$\left(\frac{g_\rho^{V^2}}{4\pi},\frac{g_\rho^T}{g_\rho^V}\right)$	$\frac{g_\omega^2}{4\pi}$	$\frac{g_\epsilon^2}{4\pi}$	$\frac{f_{\pi\Delta}^2}{4\pi}$	$\frac{f_{\rho\Delta}^2}{4\pi}$	Λ^2_{NN}	$\Lambda^2_{N\Delta}$
BSE	14.2	0.33	3.09	(0.43,6.0)	11.0	5.9	0.35	8.0	1.9	1.5
QPE	14.2	0.33	3.09	(0.43,6.8)	12.0	4.7	0.35	1.0	1.5	1.3

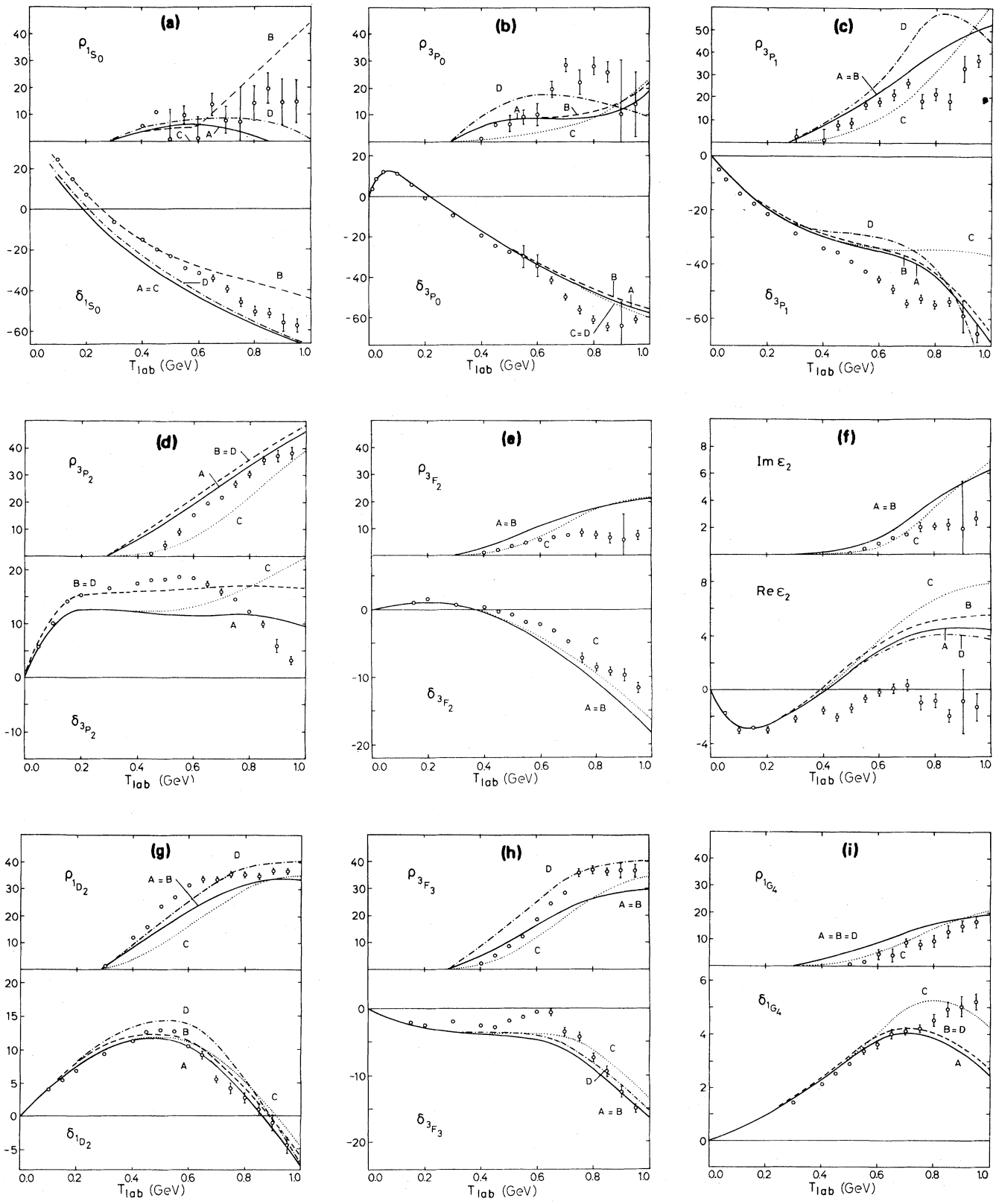

FIG. 3. Isospin 1 Bethe-Salpeter results for NN + NΔ channels (curve *A*); NN + NΔ + ΔΔ channels (curve *B*); and NN + NΔ with modified propagator of Sec. V (curve *C*). Curve *D* gives the analog of curve *A* when monopole form factors are used. It is included only when justified by a significant discrepancy with *A*. Experimental points have been taken from Ref. 39.

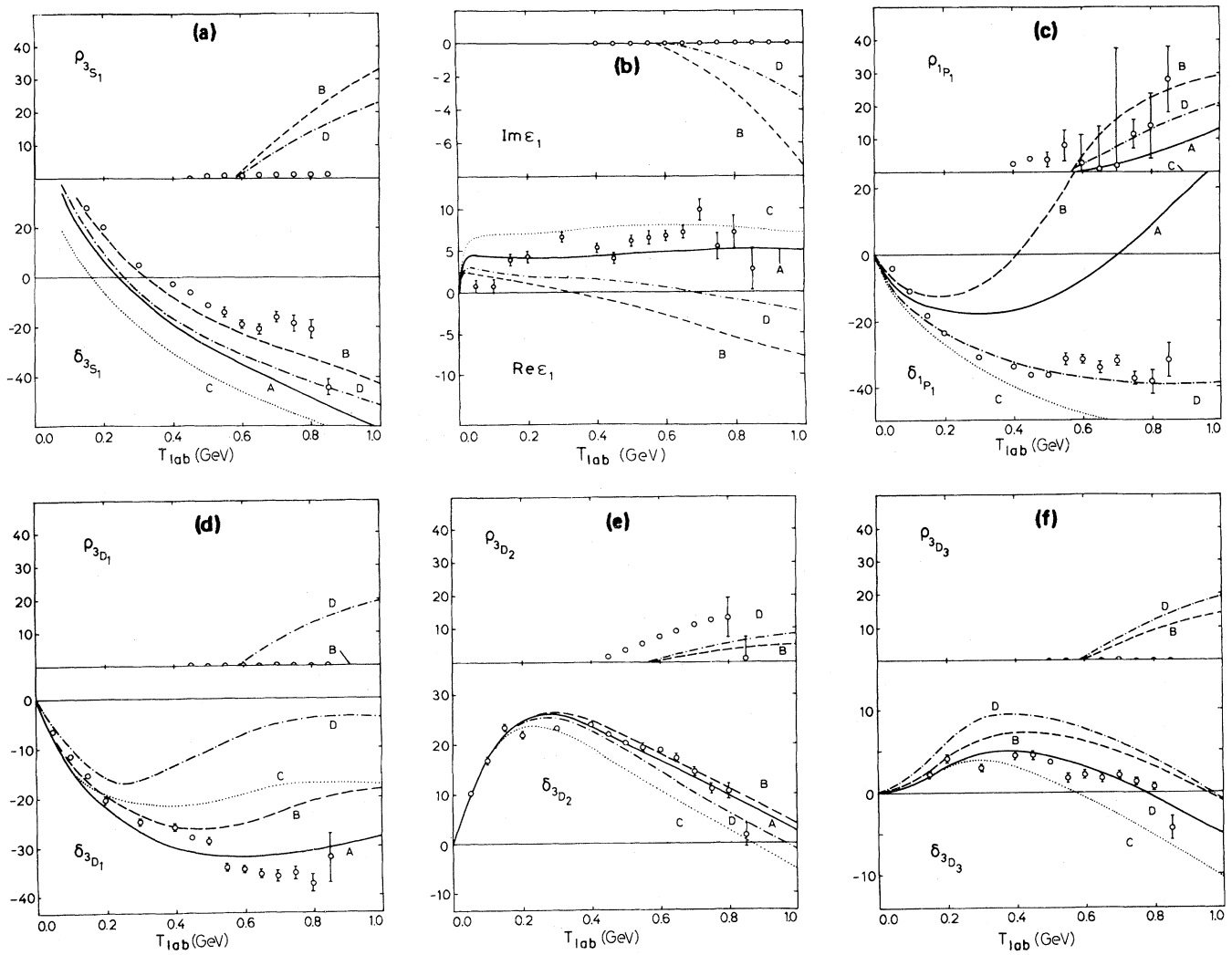

FIG. 4. Isospin 0 results from the Bethe-Salpeter equation (BSE) and the quasipotential equation (QPE) of Eq. (20). We show calculations for BSE NN only (curve *A*), BSE NN + ΔΔ (curve *B*), QPE NN only (curve *C*), and QPE NN + ΔΔ (curve *D*). Coupling constants are listed in Table III. Experimental phase shift data are taken from Ref. 39.

ρNΔ coupling. Another remarkable aspect is the fact that $^1D_2$ is too attractive in the low energy region. It turns out that this behavior cannot be remedied without spoiling predictions for *P* waves completely, and BSE clearly allows a better fit. Finally, the quasipotential equation (QPE) is seen to reproduce much better the experimental data for $^1P_1$ than BSE. It must be remarked, however, that even this large discrepancy can be largely explained from the different values of $f^2_{\rho\Delta}/4\pi$, $\Lambda_{N\Delta}$, and especially $g^2_\omega/4\pi$ (lowering $g^2_\omega/4\pi$ to the BSE value of 11, for instance, would raise the $^1P_1$ phase shift by 16 deg at 800 MeV). Therefore one should not use $^1P_1$ as a measure for the quality of a particular model.

TABLE IV. Effect of the Δ width Γ on phase shift and inelasticity. Results are from a quasipotential NN + NΔ calculation at 800 MeV. Parameters are those of Table III.

	Γ_2=176 MeV			Γ_2=100 MeV			Γ_2=40 MeV		
	Box	δ	ρ	Box	δ	ρ	Box	δ	ρ
$^1S_0$	(22;33)	−52	16	(22;33)	−51	12	(22;33)	−51	8
$^3P_1$	(2.9;3.8)	−29	44	(3.1;3.8)	−23	41	(3.2;3.7)	−17	36
$^3P_0$	(4,4;6.7)	−51	18	(4.4;6.7)	−50	19	(4.4;6.7)	−49	19
$^3P_2$	(1.2;0.64)	0	31	(1.2;0.61)	2	30	(1.3;0.57)	5	28
$^3F_2$	(0.45;0.25)	−13	16	(0.46;0.25)	−12	18	(0.48;0.26)	−11	19
ϵ_2	(0.074;0.016)	5	3	(0.054;0.008)	6	4	(0.027;0.0042)	7	4
$^1D_2$	(0.64;0.34)	1	34	(0.68;0.40)	3	37	(0.69;0.46)	5	40
$^3F_3$	(0.17;0.20)	−9	25	(0.20;0.23)	−8	29	(0.25;0.25)	−6	31

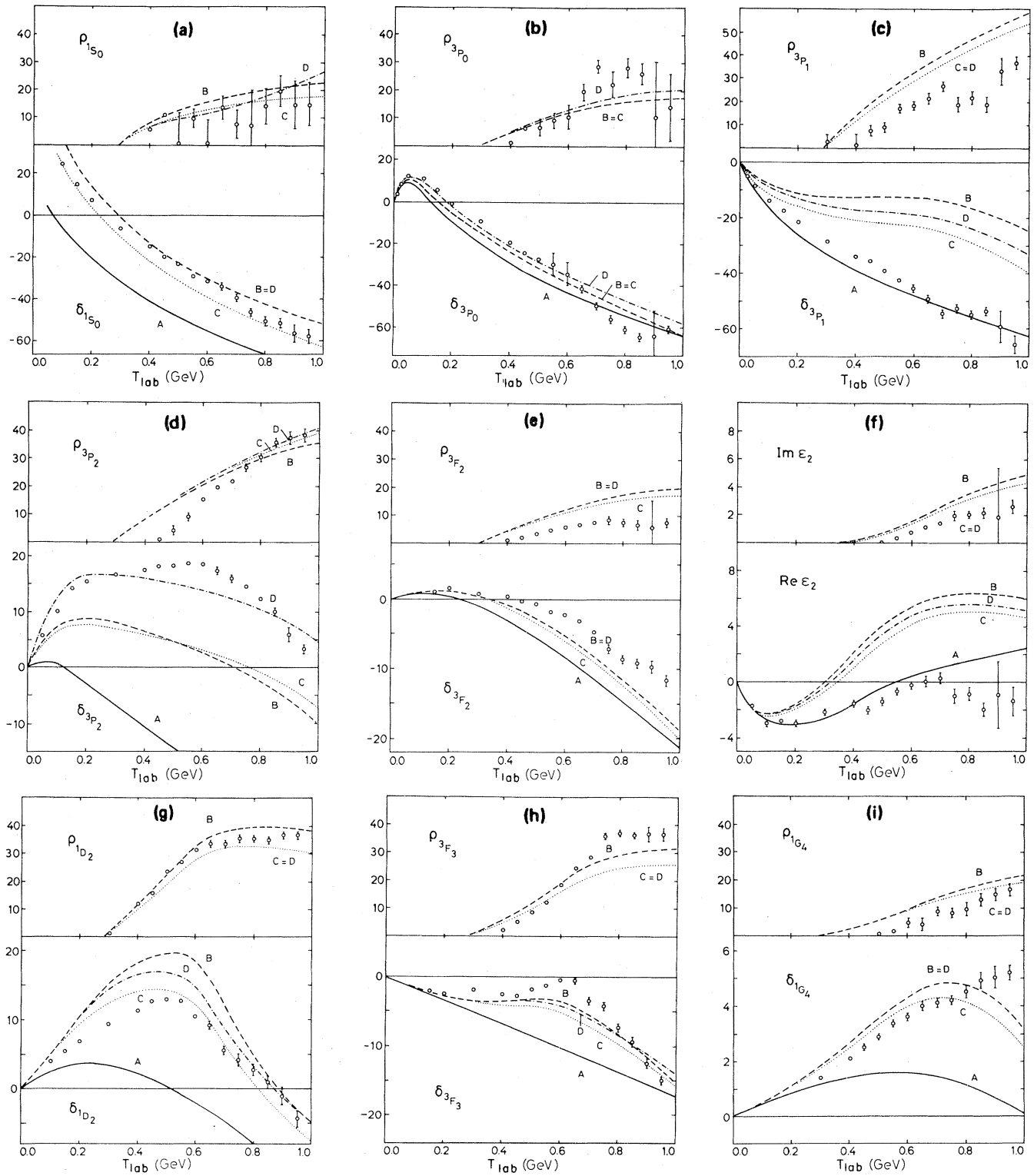

FIG. 5. Isospin 1 quasipotential results for NN only (curve *A*), NN + NΔ with ρNΔ coupled omitted (curve *B*), NN + NΔ with ρNΔ coupling included (curve *C*), and NN + NΔ + ΔΔ (curve *D*). Coupling constants are as listed in Table III. Experimental phase shift data are taken from Ref. 39.

V. SPREADING OF THE Δ WIDTH

Comparing with a three-body calculation like that of Kloet and Silbar[6] we find that our results generally predict higher inelasticities. In particular, this manifests itself clearly for the higher partial waves ($J \geq 4$). At first sight this seems to be surprising since for these channels one would expect the results to be model independent as

long as the long range pion force is included. Within the quasipotential and Kloet-Silbar model this has been studied in detail.[32] The major reason for the difference in the two models can be ascribed to the treatment of the Δ propagator. In particular, using the same Δ width description, both models yield, in general, similar results at least for the uncoupled $L=J$ high partial wave channels. The fixed mass prescription of VerWest[33,34] as has been used here tends to overestimate the inelasticity by assigning the width according to the largest possible invariant energy available for the Δ particle. To correct for this we may introduce as in the Kloet-Silbar model a momentum dependence in the Δ width. Assuming that the nucleon in the NΔ intermediate state is on mass shell, the corresponding squared invariant energy $S_{\pi N}$ available to the Δ is

$$S_{\pi N}=(2E-E_q)^2-q^2 . \tag{22}$$

The resulting q-dependent width $\Gamma_2=\Gamma_2(S_{\pi N})$ then is used in the BSE NΔ propagator. Note that this prescription is rather phenomenological and leads to conceptual difficulties if ΔΔ channels are included. A proper treatment of the πN cuts in the Δ propagator is actually required for a consistent treatment. As before, Γ_2 vanishes below pion production threshold. At higher energies Γ_2 is nonzero on a finite interval $[0,\tilde{q}]$ of the q integration only, where $\tilde{q}$ satisfies

$$S_{\pi N}=(2E-E_{\tilde{q}})^2-\tilde{q}^2=(m+\mu)^2 . \tag{23}$$

As in I, the propagators appearing in Eq. (1) are given by

$$D_2^{-1}(q_0 q)=[E+q_0-\hat{E}_2(q)+i\epsilon](E-q_0-E_q+i\epsilon) , \tag{24}$$

$$R_2^{-1}(q)=E_q+\hat{E}_2(q)-2E , \tag{25}$$

with $\hat{E}_2(q)=(m_\Delta^2+q^2)^{1/2}$, $m_\Delta=m_0-(i/2)\Gamma_2(q)$. The position of the Δ pole in the q_0 plane now has changed, but still remains in the fourth quadrant. Therefore the Wick rotation as described in I can be applied to this model without modification. Associated with this is the absence of a pole from the reduced propagator $R_2(q)$ in Eq. (23), even though $E_2(q)$ becomes real again for $q>\tilde{q}$.

The results for the variable mass Δ propagator are shown in Fig. 3 for the NN + NΔ system only. From this we see that the calculated inelasticities are smaller, especially at lower energies. In order to compare with results from other authors we select the channel $^1G_4$, which is expected to be rather insensitive to details of the model-like treatment of short range forces, regularization procedures, or truncation of the Born series to the NΔ box. From Fig. 6 we see that the agreement with the three-body calculations, at least in the low energy region, is considerably improved. Similar results have been obtained by Green and Sainio[11] when the recoil corrections were included. For higher energies fixed and variable mass results are virtually in agreement. This can be understood from the fact that at higher energies the phase parameters depend only weakly on the actual value of the width Γ_2 as has been shown in Sec. IV.

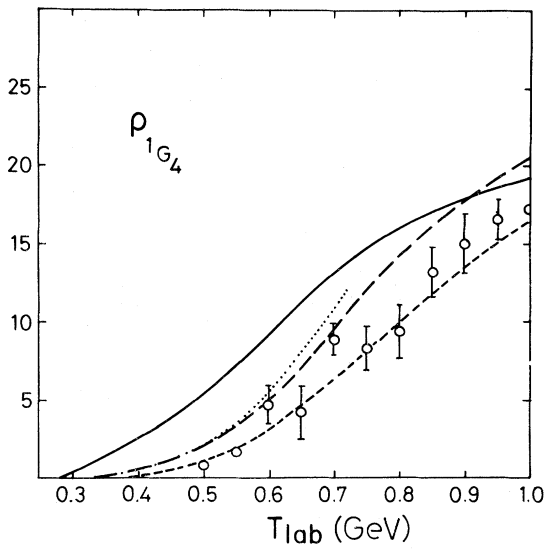

FIG. 6. Inelasticity of $^1G_4$ from various models: Graphs are, in ascending order: Ref. 6 (three body, short dashes), this work (variable mass, long dashes); Ref. 11 (fixed mass with recoil, dots); this work (fixed mass, solid line). Experimental data are from Ref. 39.

VI. CONCLUDING REMARKS

We have investigated the effect of ΔΔ channels on the phase parameters of NN scattering. Their influence is found to be small for $T=1$ channels, except for the strongly interacting S waves. This is particularly true for the inelasticities, which are dominated by the coupling to the NΔ channels. The pion production through ΔΔ states is found to be very small. For $T=0$ states, where there is no coupling to the NΔ states, the effects are accordingly larger, especially with regard to inelasticities. Similar results have been obtained using quasipotential approximation to the full BSE. Apart from having to change various coupling parameters to obtain a reasonable fit, in general it is found that the QPE results exhibit a higher sensitivity to the parameters, making the fitting process harder. In particular, the ρNΔ coupling is more strongly suppressing the resonantlike behavior of the $^1D_2$ and $^3F_3$ channels as compared to the BSE case. As a consequence the BSE allows for a better fit to the experimental phase shift analysis. However, no χ^2 fit has been tried to improve on either of the models.

The inelasticities in the various partial waves are very sensitive to how the Δ propagator is treated. Although we have attempted to include the momentum dependence of the Δ width in the N channel phenomenologically, this way leads to conceptual difficulties in the ΔΔ channel case. In a field theoretical model like the BSE, however, there is a natural way to account for these effects by summation of the series of bubble diagrams in the Δ propagator, leading to a more consistent description of the Δ width in both the NΔ and ΔΔ channels. As a consequence, since the ΔΔ production in the $T=0$ channel

plays an important role, it is expected that for this case the inelasticity may be significantly different from the ones found in this study.

ACKNOWLEDGMENTS

One of us (J.A.T.) thanks the Nuclear Theory Group and the Institute for Physical Science and Technology at the University of Maryland for the hospitality extended to him. This work received partial financial support from the "Nederlandse Organisatie voor Zuiver Wetenschappelijk Onderzoek," administered through the "Fundamenteel Onderzoek der Materie" (FOM). Partial support of the U.S. Department of Energy for this research is also gratefully acknowledged.

APPENDIX A: REDUCTION OF THE ROTATION MATRICES

The angular momentum decomposition of NN-NΔ-ΔΔ amplitudes involves integrals of the type

$$A_{ij}(\mu_1'\mu_2' \mid \mu_1\mu_2) \equiv 2\pi \int d\cos\theta_i \langle p_0 p(\theta,0)\mu_1'\mu_2' \mid \tilde{V} \mid q_0 q(0,0)\mu_1\mu_2\rangle_j d^J_{\mu\mu'}(\theta) \ , \tag{A1}$$

where $\mu_1\mu_2$ ($\mu_1'\mu_2'$) are the helicities of the incoming (outgoing) particles and $\mu \equiv \mu_1 - \mu_2$, $\mu' \equiv \mu_1' - \mu_2'$. As explained in I, Appendix A, it is possible to separate the kinematic singularities from the spinor amplitude $\tilde{V}$ in such a way that the d functions can always be written as a sum of Legendre polynomials. For $\mu \leq 2$, the relevant functions have been given in Appendix A of I. For the ΔΔ problem μ,μ' can be as large as three and the required additional functions are the following:

$$\sin^3\theta d^J_{30}(\theta) = \left[\frac{(J+3)(J+2)(J+1)}{J(J-1)(J-2)}\right]^{1/2} \left[\frac{J(J-1)(J-2)}{(2J+1)(2J+3)(2J+5)} P_{J+3} - \frac{3J(J-1)(J-2)}{(2J+1)(2J-1)(2J+5)} P_{J+1} \right.$$
$$\left. + \frac{3J(J-1)(J-2)}{(2J+1)(2J+3)(2J-3)} P_{J-1} - \frac{J(J-1)(J-2)}{(2J+1)(2J-1)(2J-3)} P_{J-3} \right] ,$$

$$\sin^2(\theta)(1+\cos\theta) d^J_{31}(\theta) = \left[\frac{(J+3)(J+2)}{(J-1)(J-2)}\right]^{1/2} \left[\frac{J(J-1)(J-2)}{(2J+1)(2J+3)(2J+5)} P_{J+3} \right.$$
$$+ \frac{(J-1)(J-2)}{(2J+1)(2J+3)} P_{J+2} - \frac{(J-1)(J-2)(J-5)}{(2J+5)(2J+1)(2J-1)} P_{J+1}$$
$$- \frac{2(J-1)(J-2)}{(2J-1)(2J+3)} P_J - \frac{(J-1)(J-2)(J+6)}{(2J+3)(2J+1)(2J-3)} P_{J-1}$$
$$\left. + \frac{(J-1)(J-2)}{(2J+1)(2J-1)} P_{J-2} + \frac{(J+1)(J-1)(J-2)}{(2J+1)(2J-1)(2J-3)} P_{J-3} \right] ,$$

$$\sin^2\theta(1-\cos\theta) d^J_{3,-1}(\theta) = \left[\frac{(J+3)(J+2)}{(J-1)(J-2)}\right]^{1/2} \left[\frac{J(J-1)(J-2)}{(2J+1()2J+3)(2J+5)} P_{J+3} \right.$$
$$- \frac{(J-1)(J-2)}{(2J+1)(2J+3)} P_{J+2} - \frac{(J-1)(J-2)(J-5)}{(2J+5)(2J+1)(2J-1)} P_{J+1}$$
$$+ \frac{2(J-1)(J-2)}{(2J-1)(2J+3)} P_J - \frac{(J-1)(J-2)(J+6)}{(2J+3)(2J+1)(2J-3)} P_{J-1}$$
$$\left. - \frac{(J-1)(J-2)}{(2J+1)(2J-1)} P_{J-2} + \frac{(J+1)(J-1)(J-2)}{(2J+1)(2J-1)(2J-3)} P_{J-3} \right] ,$$

$d^J_{3,\pm 2}$ and $d^J_{3,\pm 3}$ are absent from our algebra since we do not include ΔΔ↔NΔ or ΔΔ↔ΔΔ amplitudes.

APPENDIX B: THE Δ PROPAGATOR

Writing the Feynman rules for the coupled NΔ problem, Wick's theorem would lead to the standard expression for the free Δ propagator in x space:

$$P^{\mu\nu}(x,y) = \langle 0 \mid T\psi^\mu(x)\psi^\nu(y) \mid 0\rangle \ . \tag{B1}$$

The Fourier transform of this time ordered operator is

$$P^{\mu\nu}(q_0,\vec{q}\,)=\frac{1}{q_0-\hat{E}_q+i\eta}\sum_\sigma \Delta^\mu(\vec{q},\sigma)\bar{\Delta}^\nu(\vec{q},\sigma)-\frac{1}{-q_0-\hat{E}_q+i\eta}\sum_\sigma W^\mu(-\vec{q},\sigma)\bar{W}^\nu(-\vec{q},\sigma)\,, \tag{B2}$$

where $\sigma=\pm\frac{1}{2},\pm\frac{3}{2}$, $\hat{E}_q=(\mu_\Delta^2+q^2)^{1/2}$ and Δ and W are positive and negative energy Rarita-Schwinger wave functions, depending on $\vec{q}$ and σ only. Denoting the on-shell four-vector by $\hat{q}\equiv(\hat{E}_q,\vec{q}\,)$, the spin sums can be evaluated explicitly[35]

$$\sum_\sigma \Delta^\mu(\vec{q},\sigma)\bar{\Delta}^\nu(\vec{q},\sigma)=\frac{\hat{q}+\mu_\Delta}{2\mu_\Delta}\left[-g^{\mu\nu}+\tfrac{1}{3}\gamma^\mu\gamma^\nu+\frac{1}{3\mu_\Delta}(\gamma^\mu\hat{q}^\nu-\gamma^\nu\hat{q}^\mu)+\frac{2}{3\mu_\Delta^2}\hat{q}^\mu\hat{q}^\nu\right], \tag{B3}$$

$$\sum_\sigma W^\mu(+\vec{q},\sigma)\bar{W}^\nu(+\vec{q},\sigma)=\frac{\hat{q}-\mu_\Delta}{2\mu_\Delta}\left[-g^{\mu\nu}+\tfrac{1}{3}\gamma^\mu\gamma^\nu-\frac{1}{3\mu_\Delta}(\gamma^\mu\hat{q}^\nu-\gamma^\nu\hat{q}^\mu)+\frac{2}{3\mu_\Delta^2}\hat{q}^\mu\hat{q}^\nu\right]. \tag{B4}$$

This propagator is truncated to its positive energy contribution only, leaving us with the effective propagator used in the BSE:

$$P^{\mu\nu}(q_0\vec{q}\,)\to\frac{1}{q_0-\hat{E}_q+i\eta}\sum_\sigma \Delta^\mu(\vec{q},\sigma)\bar{\Delta}^\nu(\vec{q},\sigma)\,. \tag{B5}$$

The definition (B1) of a Green's function, however, does not lead to a covariant expression for spins higher than $\frac{1}{2}$.[36] Instead of (B1) the correct covariant propagator would be[37]

$$P^{\mu\nu}(q_0,\vec{q}\,)=\frac{q+\mu_\Delta}{q^2-\mu_\Delta^2}\left[-q^{\mu\nu}+\tfrac{1}{3}\gamma^\mu\gamma^\nu+\frac{1}{3\mu_\Delta}(\gamma^\mu q^\nu-\gamma^\nu q^\mu)+\frac{2}{3\mu_\Delta^2}q^\mu q^\nu\right]. \tag{B6}$$

Comparison of (B6) and (B5) shows that the residues at the positive energy pole are identical. We therefore basically recognize two approximations leading from (B6) to our effective propagator (B5).

(1) Restriction of the denominator in (B6) to its on-shell value: $q\to\hat{q}$.

(2) Removal of the contribution from the negative energy Δ pole by the prescription:

$$\frac{1}{q^2-\mu_\Delta^2+i\epsilon}=\frac{1}{2\hat{E}_q}\left[\frac{1}{q_0-\hat{E}_q+i\epsilon}-\frac{1}{q_0+\hat{E}_q-i\epsilon}\right]\to\frac{1}{2\hat{E}_q}\frac{1}{q_0-\hat{E}_q+i\epsilon}\,. \tag{B7}$$

In order to get an idea of the severity of these approximations we consider an extremely simplified model of the NΔ box diagram including all necessary ingredients: Consider the low energy scattering limit of the process NN$\to$N$\Delta\to$NN, where the nucleons are treated as scalar particles, coupling to a scalar meson of mass μ. The model Δ propagator is taken to be

$$P^{\mu\nu}=\frac{1}{q^2-m^2}\left[-g^{\mu\nu}+\frac{2}{3m^2}q^\mu q^\nu\right], \tag{B8}$$

where the Δ mass m is identical to the nucleon mass for simplicity. The Δ can be excited from the nucleon by a derivative coupling as in the physical case. We choose c.m. kinematics as in Fig. 7, where

$$\begin{aligned} &p_1=(E,\vec{p}\,),\quad q_1=(E+k_0,\vec{k}\,),\\ &p_1'=(E,\vec{p}\,'),\quad k_1=(-k_0,\vec{p}-\vec{k}\,),\\ &p_2=(E,-\vec{p}\,),\quad q_2=(E-k_0,-\vec{k}\,),\\ &p_2'=(E,-\vec{p}\,'),\quad k_2=(k_0,\vec{k}-\vec{p}\,')\,. \end{aligned} \tag{B9}$$

The NΔ box is proportional to the (dimensionless) integral

$$I=\frac{2\pi^2m^2}{i}\int\frac{d^4k}{(2\pi)^4}\frac{g(p,p',k)}{(q_2^2-m^2+i\epsilon)(q_1^2-m^2+i\epsilon)(\omega_{p-k}^2-k_0^2-i\epsilon)(\omega_{p'-k}^2-k_0^2-i\epsilon)}\times\text{cutoff}\,, \tag{B10}$$

where $\omega_{p-k}^2\equiv\mu^2+(\vec{p}-\vec{k}\,)^2$.

$$g=-k_1k_2+\frac{2}{3m^2}(k_1q_1)(q_1k_2)\,. \tag{B11}$$

Approximation 1 amounts to the substitution $q_1\to\hat{q}_1$ in the second term of this equation. The box integral is regularized by a monopole cutoff factor at each vertex with cutoff masses Λ_N and Λ_Δ at NNμ and N$\Delta\mu$ vertices, respectively:

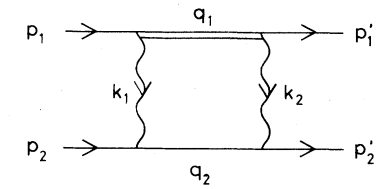

FIG. 7. Kinematics for model NΔ box diagram of Appendix B. The double line denotes the virtual Δ particle with the propagator of Eq. (B8).

$$\text{cutoff}=\frac{\Lambda_N^2-\mu^2}{\Lambda_N^2-k_1^2}\frac{\Lambda_\Delta^2-\mu^2}{\Lambda_\Delta^2-k_1^2}\frac{\Lambda_N^2-\mu^2}{\Lambda_N^2-k_2^2}\frac{\Lambda_\Delta^2-\mu^2}{\Lambda_\Delta^2-k_2^2}\ . \tag{B12}$$

Disregarding the cutoff for a moment, the k_0 integration involves the following poles:

$$\begin{aligned}&\Delta \text{ poles: } E_k-E_p-i\epsilon,\ -E_k-E_p+i\epsilon\ ,\\ &\text{N poles: } E_p-E_k+i\epsilon,\ E_p+E_k-i\epsilon\ ,\\ &\text{meson poles: } \omega_{p-k}-i\epsilon,\ -\omega_{p-k}+i\epsilon\ ,\\ &\qquad\qquad \omega_{p'-k}-i\epsilon,\ -\omega_{p'-k}+i\epsilon\ .\end{aligned} \tag{B13}$$

The integration path can be closed in the lower as well as the upper k_0 half plane at will. Choosing the lower half plane, however, will separate out the positive energy Δ pole we are interested in. Consider the low energy limit $p\to 0$. The various pole contributions then are $(I=I_\Delta+I_N+I_\mu)$.

(1) Positive energy Δ pole:

$$I_\Delta\equiv-\int\frac{d^3k}{4\pi}R(E_k-m)\frac{1}{8mE_k(m-E_k)}\ . \tag{B14}$$

(2) Negative energy N pole:

$$I_N=-\int\frac{d^3k}{4\pi}R(E_k+m)\frac{1}{8mE_k(m+E_k)}\ . \tag{B15}$$

(3) Meson poles:

$$\begin{aligned}I_\mu=\int\frac{d^3k}{4\pi}&Q(k,\mu^2,\mu^2)+\alpha^2Q(k,\Lambda_N^2,\Lambda_N^2)\\ &+\beta^2Q(k,\Lambda_\Delta^2,\Lambda_\Delta^2)-2\alpha Q(k,\mu^2\Lambda_N^2)\\ &+2\beta Q(k,\mu^2,\Lambda_\Delta^2)-2\alpha\beta Q(k,\Lambda_N^2,\Lambda_\Delta^2)\ ,\end{aligned} \tag{B16}$$

where we defined

$$R(k_0,k)\equiv\frac{m^2g(k_0,k)}{(\omega_k^2-k_0^2)^2}\left[\frac{\Lambda_N^2-\mu^2}{\Lambda_N^2+k^2-k_0^2}\right]^2\left[\frac{\Lambda_\Delta^2-\mu^2}{\Lambda_\Delta^2+k^2-k_0^2}\right]^2, \tag{B17}$$

$$Q(k,\mu_1^2,\mu_2^2)\equiv\int_\gamma\frac{dk_0}{2\pi i}\frac{m^2g(k_0k)}{[(m+E_k)^2-k_0^2][(m-E_k)^2-k_0^2]}\frac{1}{(\mu_1^2+k^2-k_0^2)}\frac{1}{(\mu_2^2+k^2-k_0^2)}\ . \tag{B18}$$

Here γ is a contour encircling only the meson poles in the lower half plane [the poles at $k_0=\pm(m\pm E_k)$ have been included already in either I_Δ or I_N]. We furthermore introduced

$$\alpha\equiv\frac{\Lambda_\Delta^2-\mu^2}{\Lambda_\Delta^2-\Lambda_N^2},\quad \beta\equiv\frac{\Lambda_N^2-\mu^2}{\Lambda_\Delta^2-\Lambda_N^2}\ . \tag{B19}$$

The sum over Q in the meson term (B16) is due to the repeated splitting off of the cutoff factors. In the low energy scattering region considered here, we expect I_Δ to be dominant. This assures us of the validity of approximation 1. The second approximation (i.e., omission of the negative energy N and Δ poles) would modify Eqs. (B14)–(B18) to

$$I'_\Delta=-\int\frac{d^3k}{4\pi}R(E_k-m)\frac{1}{8E_k^2(m-E_k)}\ , \tag{B14'}$$

$$I'_N=0\ , \tag{B15'}$$

$$I'_\mu=I_\mu \tag{B16'}$$

with a different definition of Q:

$$Q'(k,\mu_1^2\mu_2^2)\equiv\int_\gamma\frac{dk_0}{2\pi i}\frac{m^2g(k_0,k)}{4E_k^2[(m-E_k)^2-k_0^2]}\times\frac{1}{(\mu_1^2+k^2-k_0^2)(\mu_2^2+k^2-k_0^2)}\ . \tag{B18'}$$

The integrals (B14)–(B16) essentially involve 1-D integrals and were evaluated using a standard integration routine. The algebra sketched above was checked for the special case of $g(k_0,k)=1$ by comparison with results from the computer program FORMF.[38] The latter delivers numerical values of four-point functions which were seen to agree to within 10^{-2}% with $I_\Delta+I_N+I_\mu$.

Table V shows the magnitude of the various terms for representative values of meson and cutoff masses. Keeping in mind that we consider the low energy limit, we observe that I_Δ is dominant as expected. This makes approximation 1 sensible. For higher meson masses the meson pole contribution is unreliable and non-negligible, however, resulting in an error in the box diagram of about 15%. For the parameters considered the contribution

TABLE V. Effects of approximations to the Δ propagator for various representative meson and cutoff masses: $(\mu^2/m^2,\ \Lambda_N^2/m^2,\ \Lambda_\Delta^2/m^2)=(0.02,\ 1.5,\ 1.2)=$case A; $(0.02,\ 1.9,\ 1.5)=$ case B; $(0.70,\ 1.5,\ 1.2)=$ case C; I_Δ, I_N, and I_μ are the contributions to the NΔ box from Δ, N, and meson poles, respectively. For approximation 2 [see text after Eq. (B6)] there is no N pole contribution.

	A			B			C		
	I_Δ	I_N	I_μ	I_Δ	I_N	I_μ	I_Δ	I_N	I_μ
Full result	−0.814	0.002	0.095	−0.871	0.007	0.101	−0.001 32	0.000 12	0.000 15
Approx. 1	−0.814	2.2×10^{-5}	0.105	−0.871	1.1×10^{-4}	0.118	−0.001 32	1.8×10^{-6}	0.000 34
Approx. 1 + 2	−0.778		0.093	−0.828		0.102	−0.001 08		0.000 22

from the negative energy N pole I_N is negligible. This corroborates the validity of the second approximation. The influence of this approximation on the remaining I_Δ and I_μ is seen to be cancelling partially, keeping the deviation from the full result down to 5% for $\mu^2=0.02$. Again the quality of this estimate deteriorates for higher meson masses. We thus can conclude: Using the on-shell form of the model propagator instead of Eq. (B8) we tend to underestimate the "NΔ"-box diagram. The magnitude of this effect does hardly depend on the value of reasonable cutoff masses, but is seriously aggravated for higher meson masses, i.e., for the very short range part of the interaction. For reasonable values of the parameters, approximation 1 is considerably better than approximation 2 in our model. Approximation 2 has been studied before,[20] however, for the full NN problem, and turned out to be reliable in the low energy region.

---

*On leave of absence from the University of Utrecht, 3508 TA Utrecht, The Netherlands.

[1]A. M. Green, Rep. Prog. Phys. **39**, 1109 (1976).
[2]*Mesons in Nuclei,* edited by M. Rho and D. M. Wilkinson (North-Holland, Amsterdam, 1979).
[3]K. Holinde, Phys. Rep. **68**, 121 (1981).
[4]N. Hoshizaki, Prog. Theor. Phys. **60**, 1796 (1978).
[5]G. A. Yokosawa, Phys. Rep. **64**, 47 (1980).
[6]R. R. Silbar and W. M. Kloet, Nucl. Phys. **A338**, 317 (1980); Phys. Rev. Lett. **45**, 970 (1980).
[7]B. Blankleider and I. R. Afnan, Phys. Rev. C **24**, 1572 (1981).
[8]M. Araki and T. Ueda, Nucl. Phys. **A379**, 449 (1982).
[9]T.-S. H. Lee, Argonne Report, 1983; M. Betz and T.-S. H. Lee, Phys. Rev. C **23**, 375 (1981).
[10]Y. Avishai and T. Mizutani, Phys. Rev. C **27**, 312 (1983).
[11]A. M. Green and M. E. Sainio, J. Phys. G **8**, 1337 (1982).
[12]E. L. Lomon, Phys. Rev. D **26**, 576 (1982).
[13]B. J. VerWest, Phys. Rev. C **25**, 482 (1982).
[14]W. M. Kloet, J. A. Tjon, and R. R. Silbar, Phys. Lett. **99B**, 80 (1981).
[15]W. M. Kloet and J. A. Tjon, Nucl. Phys. **A392**, 271 (1983).
[16]J. A. Tjon and E. van Faassen, Phys. Lett. **120B**, 39 (1983).
[17]E. E. van Faassen and J.A. Tjon, Phys. Rev. C **28**, 2354 (1983).
[18]M. Jacob and J. C. Wick, Ann. Phys. (N.Y.) **7**, 404 (1959).
[19]H. Strubbe, Comput. Phys. Commun. **8**, 1 (1974); *ibid.* **18**, 1 (1979).
[20]M. J. Zuilhof and J. A. Tjon, Phys. Rev. C **24**, 736 (1981).
[21]J. Fleischer and J. A. Tjon, Phys. Rev. D **21**, 87 (1980).
[22]F. Gross, Phys. Rev. **186**, 1448 (1969).
[23]R. Blankenbecler and R. Sugar, Phys. Rev. **142**, 1051 (1966).
[24]R. H. Thompson, Phys. Rev. D **1**, 110 (1970).
[25]V. G. Kadychevsky, Nucl. Phys. **B6**, 125 (1967).
[26]M. H. Partovi and E. L. Lomon, Phys. Rev. D **2**, 1999 (1970).
[27]X. Bagnoud, K. Holinde, and R. Machleidt, Phys. Rev. C **24**, 1143 (1981).
[28]H. Sugawara and F. von Hippel, Phys. Rev. **172**, 1764 (1968).
[29]A. M. Green and M. E. Sainio, Nucl. Phys. **G5**, 503 (1979).
[30]R. A. Arndt and B. J. VerWest, Texas A&M Report DOE/ER/05223-29, 1981.
[31]K. Holinde and R. Machleidt, Phys. Rev. C **18**, 870 (1978).
[32]W. M. Kloet and J. A. Tjon (unpublished).
[33]B. J. VerWest, Phys. Lett. **83B**, 161 (1979).
[34]J. H. Gruben and B. J. VerWest, Phys. Rev. C **28**, 836 (1983).
[35]P. A. Carruthers, *Spin and Isospin in Particle Physics* (Gordon and Breach, New York, 1971), p. 63.
[36]S. Weinberg, Phys. Rev. **133**, B 1318 (1964).
[37]M. Veltman, in *Weak Interactions and High-Energy Neutrino Physics, International School of Physics Enrico Fermi Course XXXII, 1964,* edited by T. D. Lee (Academic, New York, 1966), p. 189.
[38]M. Veltman, FORMF, a CDC program for numerical evaluation of form factors, Utrecht, 1979.
[39]R. A. Arndt *et al.,* Phys. Rev. D **28**, 97 (1983).